UDC 551.509.313:551.511.32

A NOTE ON AN IMPROVED QUASI-LAGRANGIAN ADVECTIVE SCHEME FOR PRIMITIVE EQUATIONS

MUKUT B. MATHUR

Department of Meteorology, Florida State University, Tallahassee, Fla.

ABSTRACT

Numerical results of time integration of divergent barotropic primitive equations by a quasi-Lagrangian advective scheme, without smoothing, show that the proposed model has the desired property of conserving total energy and potential vorticity following a particle. A scheme to forecast boundary conditions in a manner similar to that in the interior is incorporated which significantly improves the results. The tests are made utilizing a large amplitude sinusoidal perturbation on a basic current as the initial state. Tests are carried out by performing the integration for 8 days.

1. INTRODUCTION

It is now being recognized from recent studies that the time integration of nonlinear primitive equations must be carried out with proper care for integral constraints of the problem. Grammeltvedt (1969) has discussed computational stability of various finite-difference analogs of so-called divergent barotropic primitive equations. He concluded that the introduction of artificial viscosity in finite-difference equations suppresses the nonlinear instability. For instance, Shuman and Vanderman (1966) were able to integrate this model by introducing a nine-point differencing scheme for nonlinear terms. Our main purpose here, however, is to develop a short-range forecast model for nonlinear primitive equations without introducing any explicit artificial viscosity in the finite-difference equations.

Leith (1965) discussed stability of one- and two-dimensional Lagrangian advective schemes for long-period time integration of a six-level primitive equation model. Økland's (1965) two-level model predicted baroclinic development with some success, but it showed irregularities in the absence of a smoothing procedure. Krishnamurti (1962) presented a time integration, carried over a period of 2 days, of the divergent barotropic primitive equations by a quasi-Lagrangian advective scheme that was computationally stable; a five-level model was used by Krishnamurti (1969) to predict the three-dimensional structure of the atmosphere in the region of the intertropical convergence zone by this scheme. In this paper, an improved form of quasi-Lagrangian advective scheme is presented which conserves total energy and potential vorticity following a particle, without any smoothing, for a period of over a week. Our scheme differs from earlier formulations (Krishnamurti 1962) mainly in the manner of treatment of the velocity fields on the northern and southern boundaries and in the use of a high-order interpolation polynomial for quasi-Lagrangian advection. A scheme to forecast the velocity field on the northern (southern) boundary in a manner similar to that in the interior, which does not involve any assumption of values outside the boundary like that of symmetry, is discussed in section 4. The introduction of a nine-point Lagrangian interpolation scheme was found to improve significantly the conservation of potential vorticity. The computational stability of this interpolation scheme is discussed in section 2. The testing of our scheme is carried out using a large-amplitude perturbation superimposed on a zonal field of geopotential (Z). Initially, zonal and meridional components of velocity are determined geostrophically. The quasi-Lagrangian advective scheme used is discussed in section 3.

2. COMPUTATIONAL STABILITY OF THE PROPOSED ADVECTIVE SCHEME

The quasi-Lagrangian advective scheme proposed for the time integration of the divergent barotropic primitive equations is based on fundamental mechanical principles of physics. It is well known that if a particle has a velocity u_1 at time t and constant acceleration $du/dt=a$, then the distance S covered by it and the velocity u_2 attained by it after a time interval Δt are

$$S=u\Delta t+\frac{1}{2}a(\Delta t)^2 \tag{1}$$

and

$$u_2=u_1+a\Delta t. \tag{2}$$

Likewise, if F is any dependent variable of the problem $dF/dt=b$,

$$F_2=F_1+b\Delta t \tag{3}$$

where b is in general a known linear function of dependent variables of the problem.

Leith (1965) discussed computational stability of the nonlinear advective terms of equation (3) for two-dimensional motion:

$$\frac{dF}{dt}=\frac{\partial F}{\partial t}+\frac{u\partial F}{\partial x}+\frac{v\partial F}{\partial y}=0 \tag{4}$$

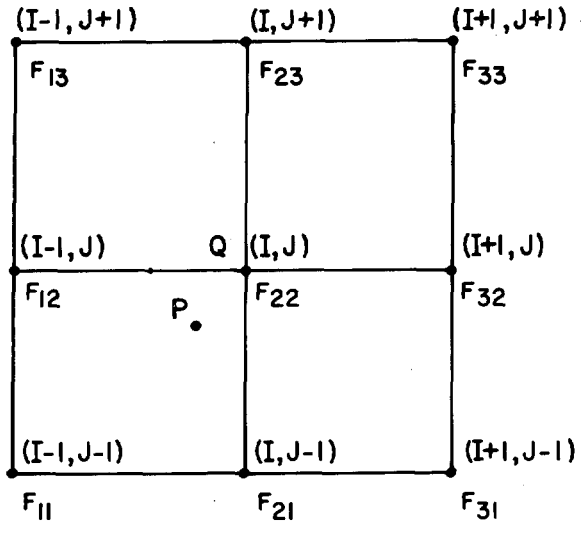

FIGURE 1.—Nine points for Lagrangian interpolation. A particle originally at P at time t arrives at Q at time $t+\Delta t$.

where u and v are components of velocity along the x and y axes, respectively.

Initially, F is known at all grid points (fig. 1). For the time integration of equation (4), use is made of equation (1) to locate position $P_{i,j}$ of the particle so that it may arrive at a grid point $Q_{i,j}$ after a time interval Δt (see section 3). Equation (2) gives future values of F_{22} as:

$$F_{22}^{n+1}=FP_{22}^{n} \tag{5}$$

where superscripts denote time steps. An interpolation scheme is required to find FP_{22}^{n}. Leith (1965) used a quadratic interpolation function:

$$F(x,y)=a+bx+cy+dx^2+ey^2. \tag{6}$$

For computational stability with the interpolation formula (6), it was necessary to advect in two steps: 1) advection along the y axis and 2) advection along the x axis starting from the result of the first step. It is shown below that a one-step advective scheme can be used if the nine-point Lagrangian interpolation (7) is used instead of interpolation (6).

A discussion of a nine-point Lagrangian interpolation will be presented here. According to this formula, a quantity F at $P(x,y)$ is given by:

$$FP=\sum_{\substack{i=I-1\\ j=J-1}}^{\substack{i=I+1\\ j=J+1}} W_{i,j}Q_{i,j} \tag{7}$$

where

$$W_{i,j}=\prod_{\substack{k=I-1\\ k\neq i}}^{k=I+1}\frac{(x-x_k)}{(x_i-x_k)}\prod_{\substack{l=J-1\\ l\neq j}}^{l=J+1}\frac{(y-y_l)}{(y_j-y_l)}.$$

The interpolation polynomial (7) reproduces the exact solution at the grid points used (fig. 1), and the error is a minimum for the points near the center (for example, see Householder 1953). Since our time step is of the order of a few minutes (linear theory), the particle at $P_{i,j}$ is always found near the center, and thus this interpolation is expected to be satisfactory. This also implies that the trajectory over which we integrate equations (1) and (2) is small, which should be the case.

Use of the interpolation polynomial (7) in (5), after some manipulation, gives:

$$\begin{aligned}F_{22}^{n+1}=&F_{22}-\frac{\gamma}{2}(F_{32}-F_{12})-\frac{\delta}{2}(F_{23}-F_{21})\\&+\frac{\gamma\delta}{4}(F_{33}-F_{31}-F_{13}+F_{11})+\frac{\gamma^2}{2}(F_{32}-2F_{22}+F_{12})\\&+\frac{\delta^2}{2}(F_{23}-2F_{22}+F_{21})+\frac{\gamma^2\delta}{4}(F_{11}-2F_{21}+F_{31}-F_{13}\\&\qquad+2F_{23}-F_{33})\\&+\frac{\gamma\delta^2}{4}(F_{11}-F_{31}-2F_{12}+2F_{32}+F_{13}-F_{33})\\&+\frac{\gamma^2\delta^2}{4}(F_{11}-2F_{21}+F_{31}-2F_{12}+4F_{22}-2F_{32}+F_{13}\\&\qquad-2F_{23}+F_{33})\end{aligned} \tag{8}$$

where all terms on the right-hand side are to be evaluated at time$=n$, $\gamma=u\Delta t/\Delta x$, and $\delta=v\Delta t/\Delta y$. Substitution of a Fourier term in equation (8) gives

$$F^{n+1}=GF^{n}=G^{n}F^{0}$$

where G is the amplification factor;

$$\begin{aligned}G=1-i[&\gamma\sin\alpha+\delta\sin\beta-\gamma^2\delta\sin\beta(1-\cos\alpha)\\&-\gamma\delta^2\sin\alpha(1-\cos\beta)]-\gamma\delta\sin\alpha\sin\beta\\&+\gamma^2(\cos\alpha-1)+\delta^2(\cos\beta-1)+\gamma^2\delta^2(\cos\alpha\cos\beta\\&\qquad-\cos\beta-\cos\alpha+1)\end{aligned}$$

where $\alpha=k_x\Delta x$, $\beta=k_y\Delta$. Here, k_x and k_y are any wave numbers in the x and the y directions, respectively.

For computational stability $|G|\leq 1$:

case 1, $\delta=0$;
$|G|^2=1+\gamma^4(\cos\alpha-1)^2+2\gamma^2(\cos\alpha-1)+\gamma^2\sin^2\alpha$,
$|G|\leq 1$ if $|\gamma|\leq\frac{1}{2}$;

case 2, $\gamma=0$;
$|G|^2=1+\delta^4(\cos\beta-1)^2+2\delta^2(\cos\beta-1)+\gamma^2\sin^2\beta$,
$|G|\leq 1$ if $|\delta|\leq\frac{1}{2}$; and

case 3, $\gamma=\delta=1$;
$|G|=1$.

It can be shown that for stability ($|G|\leq 1$),

$$|\gamma|=\left|\frac{u\Delta t}{\Delta x}\right|\leq\tfrac{1}{2}$$

$$|\delta|=\left|\frac{v\Delta t}{\Delta y}\right|\leq\tfrac{1}{2}.$$

These conditions are satisfied by the linear stability cri-

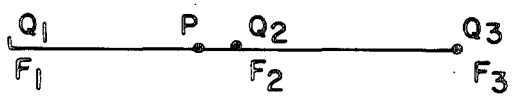

FIGURE 2.—Three points for quadratic interpolation on the northern (southern) boundary. P is the origin of the particle at time t, which arrives at Q_2 at time $t+\Delta t$.

teria (9) for the primitive equations discussed in section 3;

$$\frac{\Delta x}{\Delta t}\geq\sqrt{2}\left(\frac{u}{2}+\sqrt{gz}\right)_{max}. \tag{9}$$

In the numerical experiment, the maximum time step was estimated every hour from (9).

Boundary conditions for the divergent barotropic primitive equations are discussed in section 4 where cyclic continuity is assumed on the eastern and western boundaries. On the northern (southern) boundary, a nine-point Lagrangian interpolation scheme cannot be used, since F is not known outside this boundary. A one-dimensional second-order (quadratic) Lagrangian interpolation when substituted in (5) gives (see fig. 2):

$$F_2^{n+1}=F_2^n-\frac{\gamma}{2}(F_3^n-F_1^n)+\frac{\gamma^2}{2}(F_3^n-2F_2^n+F_1^n).$$

The amplification factor G_s was derived by Leith (1965);

$$|G_s|^2=1-\gamma^2(1-\gamma^2)(1-\cos\alpha)^2.$$

The scheme is stable if $|\gamma|\leq 1$.

For small values of α,

$$|G_s|\simeq 1-\frac{\gamma^2\alpha^4}{8}. \tag{10}$$

Use of a linear interpolation polynomial (points Q_1 and Q_2 in fig. 2) in equation (5) gives

$$F_2^{n+1}=F_1^n+\gamma[F_2-F_1].$$

The amplification factor G_L is

$$|G_L|^2=1-2\gamma(1-\cos\alpha)+2\gamma^2(1-\cos\alpha).$$

The scheme is stable if $|\gamma|\leq 1$.

For small values of α,

$$|G_L|\approx 1-\frac{1}{2}\gamma\alpha^2. \tag{11}$$

The linear interpolation scheme on the northern (southern) boundary gave better results in the time integration of our model than the quadratic interpolation. This may be partly due to the fact that the truncation error, equation (10), in amplitude for small-scale waves introduced by quadratic interpolation is smaller than that introduced by linear interpolation, equation (11); in other words, linear interpolation damps short waves more efficiently. The phase truncation error for short waves is nearly the same for both interpolation polynomials, $\simeq(\frac{1}{6})\gamma\alpha^3$ in each time step, and exceeds the amplitude truncation error in the case of quadratic interpolation.

3. NUMERICAL MODEL

Equations of motion for the two-dimensional divergent barotropic model are:

$$\frac{du}{dt}=A=fv-gm\frac{\partial z}{\partial x}, \tag{12}$$

$$\frac{dv}{dt}=B=-fu-gm\frac{\partial z}{\partial y}, \tag{13}$$

and

$$\frac{d\ln z}{dt}=C=-m\left(\frac{\partial u}{\partial x}+\frac{\partial v}{\partial y}\right) \tag{14}$$

where

$$\frac{d}{dt}=\frac{\partial}{\partial t}+m\left(u\frac{\partial}{\partial x}+v\frac{\partial}{\partial y}\right).$$

Here, u and v are components of velocity along the x (east) and y (north) axes, respectively, t is time, m is the map factor, and f is the Coriolis parameter. Initially, u, v, and z are known at all grid points. Initial values of A, B, and C are calculated from the right-hand side of equations (12), (13), and (14). For the time integration of the equations, we locate the position of the particle $(P_{i,j})$ at $t=0$ (fig. 1) so that it may arrive at a grid point $Q_{i,j}$ at $t=t+\Delta t$. The first guess for the location of $P_{i,j}$ is obtained by using equation (1);

$$xP_{i,j}^{01}=-u_{i,j}^{00}\Delta t-\frac{1}{2}A_{i,j}^{00}(\Delta t)^2$$

and

$$yP_{i,j}^{01}=-v_{i,j}^{00}\Delta t-\frac{1}{2}B_{i,j}^{00}(\Delta t)^2 \tag{15}$$

where the following notation is used to define a quantity

$$S=S_{i,j}^{n,p}\ \begin{matrix}\text{time step}\\ x\text{ coordinate}\end{matrix}\ \begin{matrix}\text{guess number}\\ y\text{ coordinate}\end{matrix}.$$

Once the location of $P_{i,j}$ is known, the values of u, v, z, A, B, and C may be interpolated at $P_{i,j}$.

A forward difference in time is carried out using equation (2);

$$u_{i,j}^{11}=uP_{i,j}^{01}+AP_{i,j}^{01}\Delta t,$$

$$v_{i,j}^{11}=vP_{i,j}^{01}+BP_{i,j}^{01}\Delta t,$$

and

$$\chi_{i,j}^{11}=\chi P_{i,j}^{01}+CP_{i,j}^{01}\Delta t \tag{16}$$

where

$$\chi=\ln z.$$

$A_{i,j}^{11}$, $B_{i,j}^{11}$, and $C_{i,j}^{11}$ are evaluated from equations (12), (13), and (14), respectively, and a second guess for the location of $P_{i,j}^{02}$ is obtained using equation (1). Thus,

$$xP_{i,j}^{02}=-uP_{i,j}^{01}\Delta t-\frac{1}{2}AP_{i,j}^{01}(\Delta t)^2$$

and

$$yP_{i,j}^{02}=-vP_{i,j}^{01}\Delta t-\frac{1}{2}BP_{i,j}^{01}(\Delta t)^2. \tag{17}$$

Interpolation yields the values of $uP^{02}_{i,j}$, $vP^{02}_{i,j}$, $\chi P^{02}_{i,j}$, $AP^{02}_{i,j}$, $BP^{02}_{i,j}$, and $CP^{02}_{i,j}$. An implicit time-differencing scheme may now be used to obtain:

$$u^{12}_{i,j}=uP^{02}_{i,j}+\frac{1}{2}(AP^{02}_{i,j}+A^{11}_{i,j})\Delta t,$$

$$v^{12}_{i,j}=vP^{02}_{i,j}+\frac{1}{2}(BP^{02}_{i,j}+B^{11}_{i,j})\Delta t,$$

and (18)

$$\chi^{12}_{i,j}=\chi P^{02}_{i,j}+\frac{1}{2}(CP^{02}_{i,j}+C^{11}_{i,j})\Delta t,$$

and the corresponding accelerations can be obtained from equations (12), (13), and (14).

An implicit iterative scheme is introduced at this stage, utilizing the nth guess for u, v, and z at time $(t+\Delta t)$. The new guess defining the position of particle $P_{i,j}$ at time (t) is given by

$$xP^{0,n+1}_{i,j}=-\frac{1}{2}(uP^{0n}_{i,j}+u^{1n}_{i,j})\Delta t$$

and (19)

$$yP^{0,n+1}_{i,j}=-\frac{1}{2}(vP^{0n}_{i,j}+v^{1n}_{i,j})\Delta t.$$

Equations (19) are a combination of equations (1) and (2). The corresponding velocities are obtained using equations (18), that is,

$$u^{1,n+1}_{i,j}=uP^{0,n+1}_{i,j}+\frac{1}{2}(AP^{0,n+1}_{i,j}+A^{1n}_{i,j})\Delta t$$

and (20)

$$v^{1,n+1}_{i,j}=vP^{0,n+1}_{i,j}+\frac{1}{2}(BP^{0,n+1}_{i,j}+B^{1n}_{i,j})\Delta t.$$

Since we now have the $(n+1)$ guess for $P_{i,j}$, u, v, and z, equations (18) and (19) can be iterated. Numerical integrations were carried out for a period of 24 hr using one, three, five, and seven scans. The results were similar. Small-scale irregularities developed after 8 days of integration with one scan. Similar results were obtained when three scans were used. Numerical results with one scan are presented in section 5.

4. INITIAL AND BOUNDARY CONDITIONS OF A TEST EXPERIMENT

The initial field of z is defined as

$$z(x, y, 0)=\bar{z}(y)+100\cos\frac{2\pi x}{\lambda}\sin^2\frac{y-y_0}{y_M-y_0}\pi \qquad (21)$$

where the first term on the right represents a geopotential field in geostrophic balance and the second term a perturbation superimposed in the x and y directions. In (21) y_M and y_0 are y coordinates of the northern and southern boundaries, respectively. The initial fields of u and v are determined assuming geostrophic balance.

For the purpose of forecasting on the boundary, cyclic continuity is assumed on the eastern and western boundaries. In the following, our scheme for forecasting on the northern and southern boundaries is presented. Since $v=0$ initially at all points on these boundaries, the particle that lies at point P (fig. 2) at $t=0$ so as to reach a grid point Q_2 after time $t=\Delta t$ can be either to the east or west of Q_2, and the position of P can be determined from equation (1). The interpolating polynomial for determining values of variables u, v, etc. at P on the boundary was discussed in section 2. New values of u at Q_2 are found from equation (2), and z is evaluated assuming geostrophic balance.

Since at Q_2

$$\left(\frac{dv}{dt}\right)_{t=\Delta t}=\left(-fu-g\frac{\partial z}{\partial y}\right)_{t=\Delta t}=0$$

if v and B are both zero initially at all points on the northern (southern) boundary, they will remain zero for all time. To evaluate C at Q_2 on the northern (southern) boundary (which involves values across the boundary, see equation (14)), use is made of equation (18), since z at P at $t=0$ and z at Q_2 at $t=\Delta t$ are known. An iterative scheme similar to that in the interior can be used on the northern (southern) boundary, if geostrophy is assumed, to determine z, and (18) is used to determine C. This iterative scheme significantly improved our results. These boundary conditions imply that equations (12) through (14) should conserve total energy, total mass, and potential vorticity following a particle.

5. NUMERICAL RESULTS

The initial field of z given by equation (21) is shown in figure 3A, and the corresponding field of potential vorticity in figure 4A. The southern boundary is at 30° N. and the northern at 45° N. The maximum in potential vorticity in the trough is 5.0×10^{-8} m^{-1} sec^{-1}, and the minimum in the ridge is about 2.0×10^{-8} m^{-1} sec^{-1}. A separate maximum in potential vorticity (4.9×10^{-8} m^{-1} sec^{-1}) is located in the extreme northwestern portion of the grid, and a minimum south of the trough. Figures 3B and 3C give the field of z after 4 and 8 days, respectively, and figures 4B and 4C give the same for potential vorticity. The field of z, which is quite smooth in figure 3B, shows small-scale irregularities after 8 days of integration near the northern and southern boundaries (fig. 3C), though it is still smooth in the interior. During the next 48 hr (not shown), this small-scale feature propagates inward, though the large-scale feature still remains distinct.

Persistence of the maxima and minima in figures 4A to 4C indicates that the model does conserve potential vorticity following a particle. Figure 5 shows the variation of total energy and mean potential vorticity with time, and their values on each day are listed in table 1. The largest variation in total energy on any day is within 0.1 percent and in mean potential vorticity within 2 percent. Even after 8 days, no appreciable change is observed in

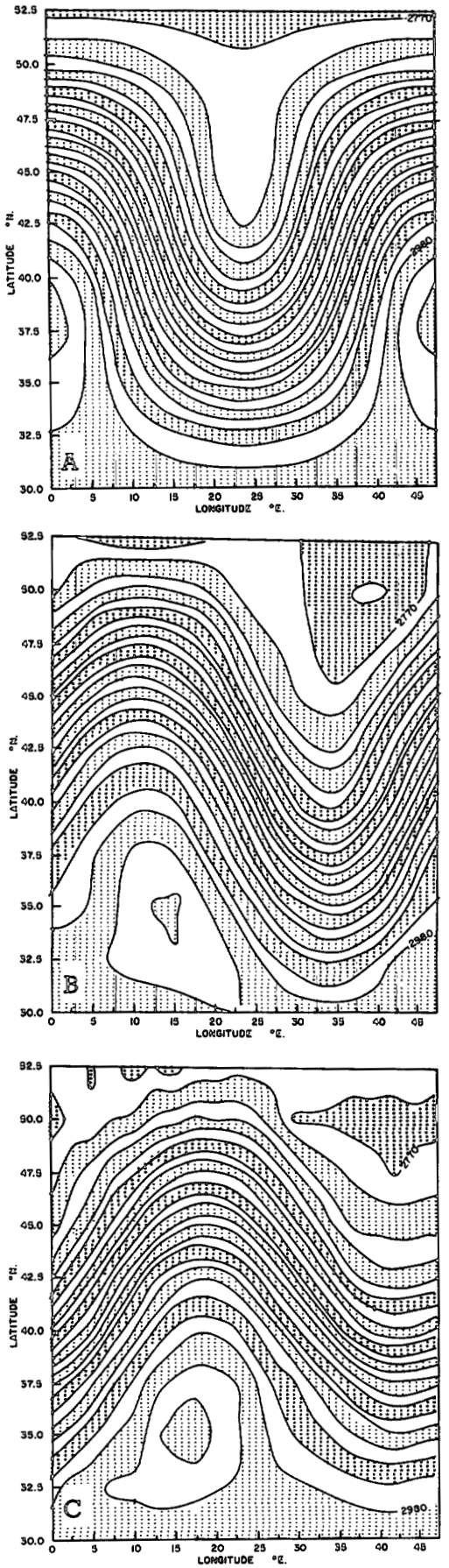

FIGURE 3.—(A) initial distribution of height of the free surface (Z); (B) the forecast field of Z at 4 days; and (C) the forecast field of Z at 8 days. Isolines are labeled in meters; the shading interval is 10 m.

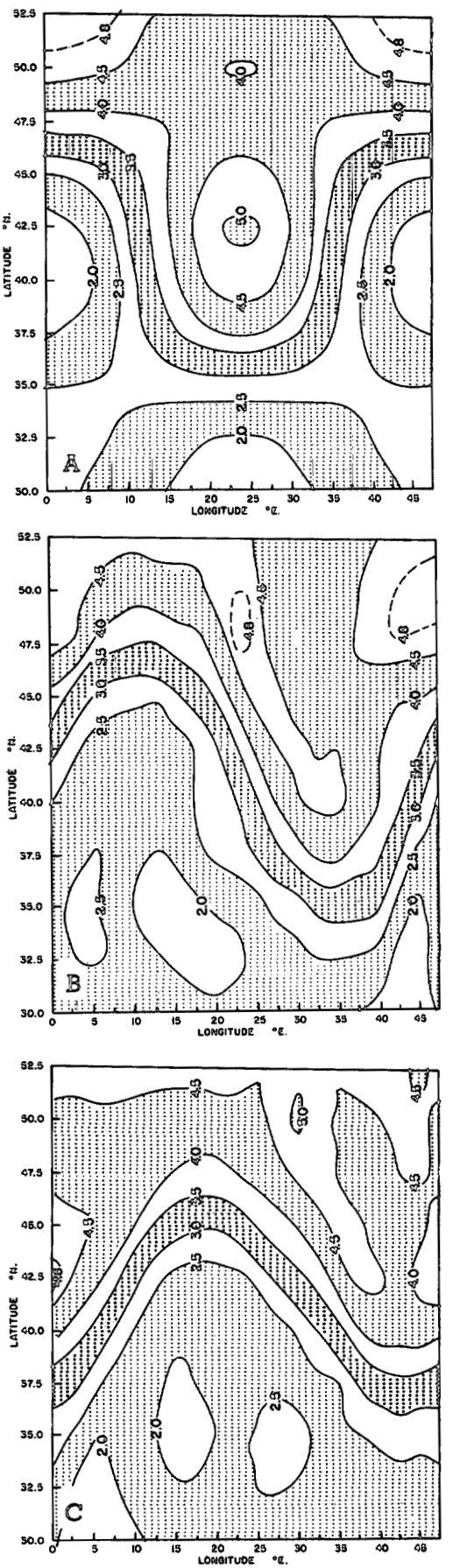

FIGURE 4.—(A) initial distribution of potential vorticity; (B) the distribution of potential vorticity at 4 days; and (C) the distribution of potential vorticity at 8 days. Isolines are labeled in 10^{-8} m^{-1} sec^{-1}.

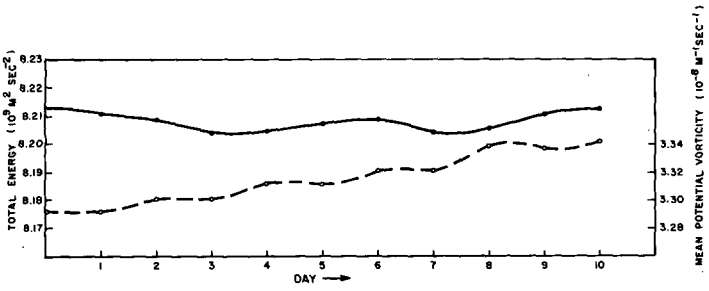

FIGURE 5.—Variation of total energy (solid line) and mean potential vorticity (dashed line) with time. Maximum variation in total energy is of the order of 0.1 percent and in mean potential vorticity less than 2 percent.

TABLE 1.—*Mean potential vorticity (Q), total energy (E), and root-mean-square divergence (D) as a function of time*

Day	Q (10^{-8}m^{-1}sec^{-1})	E (10^{9}m^{2}sec^{-2})	D (10^{-7}sec^{-1})
0	3.2908	8.2132	----------
1	3.2912	8.2113	4.8697
2	3.2985	8.2090	5.0359
3	3.3006	8.2044	4.1578
4	3.3106	8.2051	4.1430
5	3.3107	8.2071	4.6880
6	3.3205	8.2093	4.2749
7	3.3256	8.2042	3.1180
8	3.3392	8.2061	4.5193
9	3.3376	8.2101	3.8757
10	3.3420	8.2127	4.6244

these quantities. The last column in table 1 gives the root-mean-square divergence, which shows little variation and remains small throughout the integration period. Shuman and Vanderman (1966) considered this desirable for computational stability.

6. CONCLUSION

The numerical results presented show that the proposed quasi-Lagrangian advective scheme can be used for time integration of the two-dimensional divergent barotropic primitive equations for a period of over a week without smoothing. The advective scheme used conserves total energy and potential vorticity following a particle. One significant advantage of this formulation is that we need not calculate nonlinear terms explicitly (in finite-difference form). Since large-scale motions are quasi-horizontal, it is conceptually possible to extend the use of the above model to time integration of the three-dimensional primitive equations, assuming that nonlinear effects involving vertical motion are not large. We shall present the results of such a study for a fine-mesh primitive equation model in a subsequent paper.

ACKNOWLEDGMENTS

The author was first introduced to the quasi-Lagrangian advective scheme by Professor T. N. Krishnamurti. His guidance and encouragement throughout this study are gratefully acknowledged. He had also the benefit of many discussions with Professor J. O'Brien who also read a first draft of the paper and gave several useful comments. The author expresses his appreciation to Mr. W. E. Fuller of the computational facility at Florida State University, who helped in coding the program, and to the computational facility for providing the computing time. Financial support for this work was received from the Atmospheric Science Section, National Science Foundation, NSF Grant GA-1480 and the Department of Defense Themis Contract No. DAAB-07-69-C-0062.

REFERENCES

Grammeltvedt, Arne, "A Survey of Finite-Difference Schemes for the Primitive Equations for a Barotropic Fluid," *Monthly Weather Review*, Vol. 97, No. 5, May **1969**, pp. 384–404.

Householder, Alston S., *Principles of Numerical Analysis*, McGraw-Hill Book Co., Inc., New York, **1953**, 274 pp., (see pp. 185–206).

Krishnamurti, T. N., "Numerical Integration of Primitive Equations by a Quasi-Lagrangian Advective Scheme," *Journal of Applied Meteorology*, Vol. 1, No. 4, Dec. **1962**, pp. 508–521.

Krishnamurti, T. N., "Experiment in Numerical Prediction in Equatorial Latitudes," *Quarterly Journal of the Royal Meteorological Society*, Vol. 95, No. 405, July **1969**, pp. 594–620.

Leith, C. E., "Lagrangian Advection in an Atmospheric Model," *Technical Note* No. 66, World Meteorological Organization, Geneva, **1965**, pp. 168–176.

Økland, Hans, "An Experiment in Cyclogenesis Predicted by a Two-Level Model," *Monthly Weather Review*, Vol. 93, No. 11, Nov. **1965**, pp. 663–672.

Shuman, Frederick G., and Vanderman, Lloyd W., "Difference System and Boundary Conditions for Primitive-Equation Barotropic Forecast," *Monthly Weather Review*, Vol. 94, No. 5, May **1966**, pp. 329–335.

[*Received August 18, 1969*]